UNIVERSIDAD DISTRITAL
FRANCISCO JOSÉ DE CALDAS

Research

Modeling a Fixed-Bed System with Coal Volatiles Post-Combustion for Ceramic Kiln Firing

Modelamiento de un sistema de lecho fijo con poscombustión de volátiles del carbón para hornos de cocción de cerámicos

Marco A. Ardila-Barragán[1] ID, María del Pilar Triviño-Restrepo[1] ID, Luis F. Lozano-Gómez[1] ID, Naren N. Ardila-Otálora[1] ID ✉[*], Brigith D. Cruz-Molina[1] ID, Fabián R. Jiménez-López[1] ID, Alfonso López-Díaz[1] ID, and Jaime A. Riaño-Villamizar[2]

[1]Universidad Pedagógica y Tecnológica de Colombia ROR (Tunja, Colombia).
[2]Inversiones Ladrillos Maguncia SAS (Sotaquirá-Boyacá, Colombia).

Abstract

Context: It is estimated that, in Colombia, more than 1300 brick industries consume around 5800 Tcal/year, which are supplied by coal, biomass, wood, and gas combustion. The most commonly used kilns are down-draught, wherein coal combustion is produced on fixed-grate beds, emitting greenhouse gases and other pollutants. As a contribution to solving this problem, this work presents the model of a fixed-bed system with coal volatiles post-combustion.

Method: Temperature, time, coal consumption, and combustion products were monitored in a down-draught kiln, in order to determine their mass, energy, and thermal efficiency balances. Coal characterization was performed under ASTM standards, ashes were determined via XRD, XRF, and TGA, and emissions were obtained using a gas analyzer. The thermodynamic model used to design the 3D reactor was based on coal-burning analysis.

Results: The process lasted 3166 min, consuming 2150 kg of coal. The combustion gases exhibited a varying composition of CO_2, CO, O_2, and hydrocarbons. The temperature on the grate reached 900 °C, and we recorded 1000 °C in the dome and 600 °C at the chimney base. The temperature difference between the dome and the chimney base explains the heat transferred for ceramic baking. The calorific value of the char was 19.52 % higher than that of the coal used. The composition of the ash showed silicon oxide, mullite, and goethite. The 3D model consists of a grate with preheater ducts for the secondary air post-combustion of the volatiles.

Conclusions: The outcome of this research was the 3D model of a fixed-bed grate for coal combustion and volatiles post-combustion. With its implementation, we expect to improve air quality and reduce the effects of the process on human health, as well as its operating costs.

Keywords: secondary air, ceramic firing, coal combustion, down-draught kiln, fixed-bed grill, post-combustion

*✉ **Correspondence:** naren.ardila@uptc.edu.co

Resumen

Contexto: Se estima que, en Colombia, más de 1300 industrias ladrilleras consumen alrededor de 5800 Tcal/año, provenientes de la combustión de carbón, biomasa, leña y gas. Los hornos más comunes son los de tiro descendente, en los cuales la combustión del carbón se realiza sobre parrillas fijas, emitiendo gases de efecto invernadero y otros contaminantes. Como contribución a la solución de este problema, este trabajo presenta el modelo de un sistema de lecho fijo con poscombustión de volátiles del carbón.

Método: Se monitorearon la temperatura, el tiempo, el consumo de carbón y los productos de combustión en un horno de tiro descendente, a fin de determinar los balances de masa, energía y eficiencia térmica. La caracterización del carbón se realizó bajo las normas ASTM, las cenizas se analizaron mediante XRD, XRF y TGA, y las emisiones se determinaron utilizando un analizador de gases. El modelo termodinámico empleado para el diseño del reactor 3D se basó en el análisis de la combustión del carbón.

Resultados: El proceso tuvo una duración de 3166 minutos, con un consumo de 2150 kg de carbón. Los gases de combustión presentaron una composición variable de CO_2, CO, O_2 e hidrocarburos. La temperatura en la parrilla alcanzó los 900 °C, y se registraron 1000 °C en la cúpula y 600 °C en la base de la chimenea. La diferencia de temperatura entre la cúpula y la base de la chimenea explica el calor transferido para la cocción de la cerámica. El poder calorífico del char fue 19.52 % superior al del carbón utilizado. La composición de las cenizas mostró la presencia de óxido de silicio, mullita y goethita. El modelo 3D consiste en una parrilla con conductos precalentadores para el aire secundario destinado a la poscombustión de los volátiles.

Conclusiones: El resultado de esta investigación fue el modelo 3D de una parrilla de lecho fijo para la combustión de carbón y la poscombustión de volátiles. Con su implementación, se espera mejorar la calidad del aire y reducir los efectos del proceso sobre la salud humana, así como sus costos operativos.

Palabras clave: aire secundario, cocción de cerámicos, combustión de carbón, hornos colmena, parrilla de lecho fijo, poscombustión

Table of contents

1. Introduction

In 2016, China contributed significantly to global brick production, accounting for 54of the total output, followed by India (11 %), Pakistan (8 %), Bangladesh (4 %), and the rest of the world (23 %) (1). For the 2020-2025 period, the compound annual growth rate was expected to exceed 3 % (2). In 2015, Colombia reported a production of more than 10 Mt of fired clay, with an annual energy consumption ranging from 5 to 7 Tcal. This energy supply was obtained mainly from coal (62-71 %), wood (20-25 %), coal-biomass mixtures (7 %), and gas (0.00172-3 %). The production process is carried out at diverse scales, in artisanal, semi-merchandized artisanal, small, medium, and large-scale enterprises (3).

The most commonly used artisanal kilns in Colombia and other Latin American countries are of the beehive and trench types (4), where coal combustion takes place in fireboxes (3) equipped with a fixed-bed grate. These systems emit greenhouse gases and other pollutants (CO_2, CO, SO_2, CXHY, NOX, $PM_{2,5}$, and PM_{10}). Such contaminants pose health risks to the local population and the surrounding environment, and their environmental impacts have led to the implementation of increasingly stringent regulations aimed at reducing the deterioration of ecosystems (5–8).

Coal combustion in a fixed bed at atmospheric pressure is carried out without control over the amount of air supplied, an issue that is further complicated by the lack of homogeneity in the fuel particle size. Another peculiarity is that the heating of the load occurs at a low rate, promoting the release of uncombusted volatiles, leading to their direct emission into the environment in the form of soot (9).

To improve the productivity of the brickmaking sector, various technologies have been proposed, which are aimed at improving the energy efficiency of the aforementioned kilns, decreasing coal consumption, and reducing pollutant emission levels (10). These improvements can be achieved through the implementation of technological upgrades, such as the mechanization and automation of the process. In this vein, our research focused on the development of the 3D model of a solid carbonaceous material combustion system with volatiles post-combustion (SCMCS-VPC), designed for artisanal kilns with fixed-bed grates used for ceramic firing.

2. Material and methods

This research consisted of an experimental study for the development of the SCMCS-VPC, with the purpose of minimizing the emission of volatiles generated during the ceramic firing process (10) in inverted-flame beehive-type kilns (11) equipped with a fixed-bed grate which utilize coal combustion (Fig. 1). The fieldwork was conducted at the Maguncia brick industry, located in the jurisdiction of Sotaquirá, and at ceramic handicraft factories in the municipality of Ráquira, both in the department of Boyacá. The project was executed in three phases.
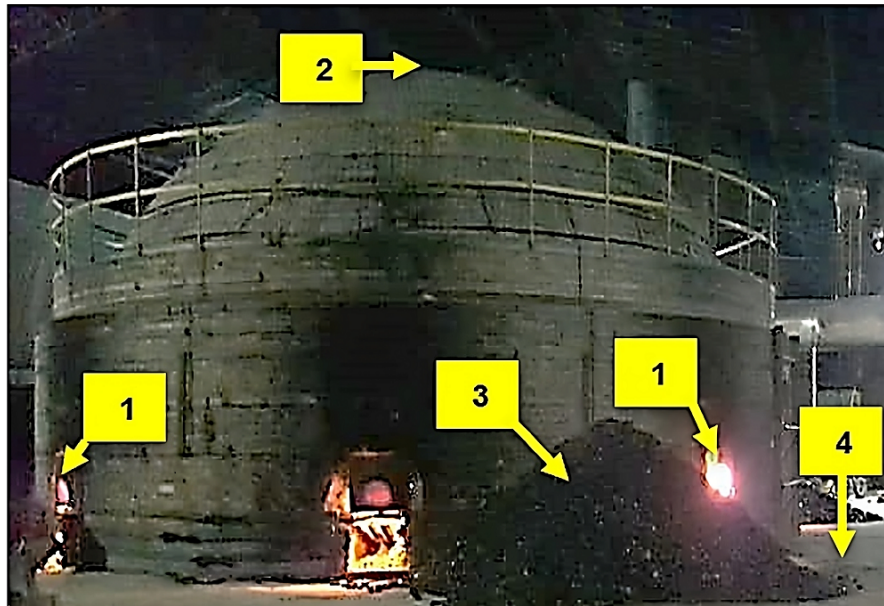
Figure 1. Sampling points for charge and temperature monitoring in an inverted-flame beehive kiln. 1: Burners 1 and 2; 2: dome thermocouple; 3: coal feed pile; 4: chimney-based thermocouple

2.1.   Phase I: field data collection

This phase involved characterizing the coal through the ASTM's standard procedures; the analysis of solid combustion products using DRX, FRX, and TGA techniques; and the monitoring of the combustion process via temperature recording with type-K thermocouples and a data logger, which was complemented by photography and video documentation. The fuel supply was weighed on a digital scale with a precision of 0.1 kg, and the composition of the gaseous emissions was determined using an E Instruments E8500 Plus analyzer. Based on this information, the operating parameters were established in order to calculate the mass and energy balance.

2.2.   Phase II: mass balance, energy balance, and thermal efficiency calculations

The combustion process for ceramic firing in an inverted flame beehive kiln is analytically described in Eq. (1), which represents the mass and energy balances.

$$C_{TSm} + \text{air} + E_{Ign} = E_{Gen} + G_{chm} + Cnz_{acm} + C_{inq} \tag{1}$$

where:

- C_{TSm} = total coal supplied to the firing process

- E_{Ign} = ignition energy

- E_{Gen} = thermal energy generated by combustion

- G_{chm} = chimney gases

- Cnz_{acm} = ashes accumulated during firing

- C_{inq} = unburned coal

C_{TSm} corresponds to the sum of the partial loads fed into each burner. The total burned coal (C_{Tqm}) is calculated using Eq. (2).

$$C_{Tqm} = C_{TSm} - H_{Hum} - Cnz_{acm} - V_{CxHy} - C_{inq} \tag{2}$$

where:

- H_{Hum} = moisture in the total coal supplied

- V_{CxHy} = volatile compounds

The composition of G_{chm}, which was determined by means of the combustion analyzer, is expressed in Eq. (3).

$$G_{chm} = CO_2 + V_{CxHy} + CO + O_2 + N_2 \tag{3}$$

The accumulated ashes (Cnz_{acm}), defined in Eq. (4), consist of the ashes from the total burned coal (Cnz_{CTqm}) and C_{inq}.

$$Cnz_{acm} = Cnz_{CTqm} + C_{inq} \tag{4}$$

The percentage of unburned coal in the ashes ($\%C_{inq}$) is calculated via Eq. (5).

$$\%C_{inq} = \frac{C_{inq}}{Cnz_{acm}} \times 100 \tag{5}$$

The energy balance is calculated using Eqs. (6) to (9).

$$E_T = E_{Tent} - E_{Tsld} \tag{6}$$

$$E_{Tent} = E_{C_{TSm}} + E_{Ign} \tag{7}$$

$$E_{Tsld} = E_{C_{Tqm}} + E_{C_{inq}} \tag{8}$$

$$E_T = \left(E_{C_{TSm}} + E_{Ign} \right) - \left(E_{C_{Tqm}} + E_{C_{inq}} \right) \tag{9}$$

where:

- E_T = total energy

- E_{Tin} = total energy input

- E_{Tout} = total energy output

- $E_{C_{TSm}}$ = total energy from the supplied coal

- E_{Ign} = ignition energy

- $E_{C_{Tqm}}$ = energy from the total burned coal

- $E_{C_{inq}}$ = energy from the total unburned coal

Energy is determined as a function of heat (Q) and mass, as shown in Eq. (10).

$$Q = m_{C_{Tqm}} * VC \tag{10}$$

where:

- $m_{C_{Tqm}}$ = total mass of burned coal
- VC = calorific value

The thermal efficiency (η) of the combustion process for ceramic firing in the beehive kiln corresponds to the ratio between $E_{C_{Tqm}}$ and $E_{C_{TSm}}$. This is calculated by means of Eq. (11).

$$\eta = \frac{E_{C_{Tqm}}}{E_{C_{TSm}}} = \frac{Q_{C_{Tqm}}}{Q_{C_{TSm}}} \tag{11}$$

where:

- $Q_{C_{Tqm}}$ = heat from total coal burned
- $Q_{C_{TSm}}$ = heat from total coal supplied

The heat from the total burned coal ($Q_{C_{Tqm}}$) is obtained from Eq. (10), while the heat supplied ($Q_{C_{TSm}}$) is calculated via Eq. (12).

$$Q = m_{C_{TSm}} * VC \tag{12}$$

where:

- $m_{C_{TSm}}$ = Mass of the total coal supply

2.3. Phase III: thermodynamic and 3D modeling

Thermodynamic modeling was performed based on the analysis of the burned coal (12) from burners equipped with a fixed-bed grate, where the air enters through the lower section of the kiln and passes through the fuel (Fig. 2). This process operates with the kiln door open, and air is regulated empirically by adjusting the chimney draft. Consequently, it is not possible to control combustion under stoichiometric parameters. Hence, black smoke emissions are generated from chimneys, indicating an incomplete combustion and energy losses due to unburned volatile hydrocarbons (9, 13), which may lead to severe pollution issues. For the reactor design (Fig. 3), we employed the French method for product designed (14).

The baseline was set as follows: air temperature: 25 °C; average autoignition temperature of the low-rank coal: 250 °C (15); ignition temperature of the volatiles: 400 °C.

2.3.1. 3D modeling

Based on the thermodynamic modeling and the fuel consumption curves, we calculated the stoichiometry of the combustion of 5 kg of coal with 30 % excess air (16). From the results obtained, the grate area, the air flow, and the dimensions and distribution of the ducts were determined, along with the required primary and secondary air supplies. Finally, the 3D model was created, using SolidWorks to design the components, assemble the complete system, and generate manufacturing drawings.
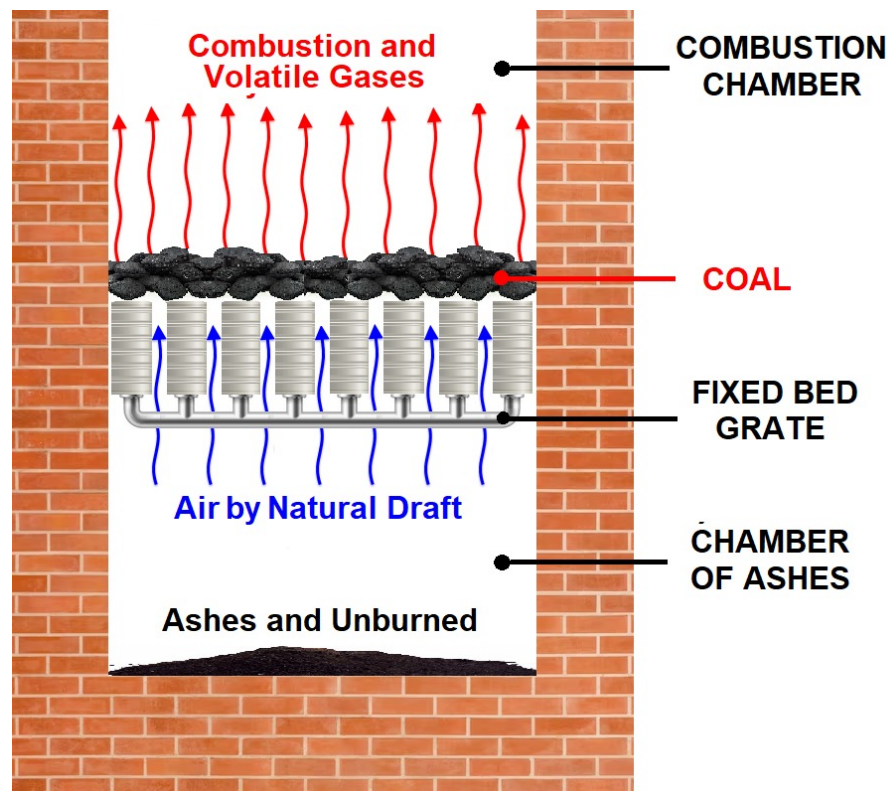
Figure 2. Schematic representation of the coal combustion process in a fixed-bed grate burner

3.   Results

3.1.   Technical and technological description of the firing process

The firing of the ceramic load in the beehive kiln was achieved through the heat generated during the combustion of coal in fireboxes equipped with a fixed-bed grate. The total coal supply, as a function of time, is shown in Fig. 4.

The total duration of the firing process was 52.76 h (3166 min), with a coal consumption of 2.15 t, supplied in 23 kg batches, with incremental increases averaging 1 kg at 35 min intervals. This procedure was maintained until the maximum gas temperatures were reached: 1050 °C in the dome, and 637 °C at the base of the chimney. It can be inferred that the heat difference between these two points corresponds to the energy consumed during the ceramic firing process, as well as to heat and convection losses through the kiln walls.

3.2.   Characterizing the coal and solid combustion products

Sampling of the coal and solid combustion products (ashes and unburned material) was conducted in two fireboxes. The results of this characterization are presented in Table **I**.
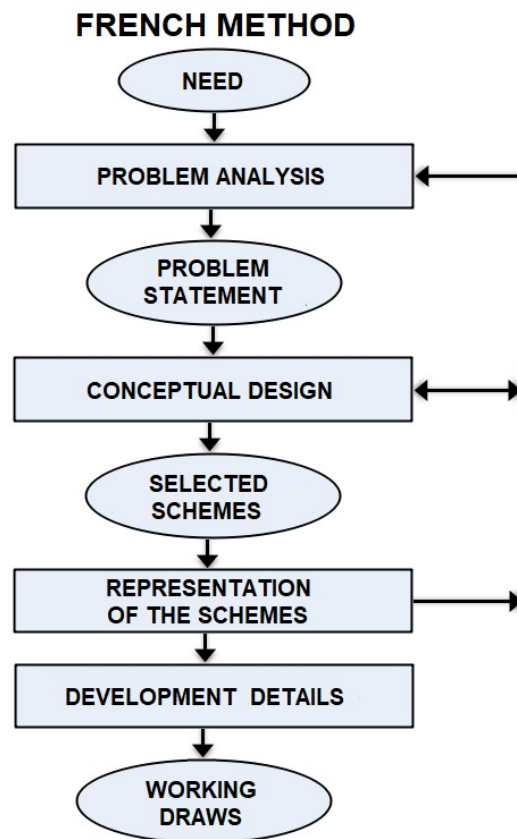
FRENCH METHOD

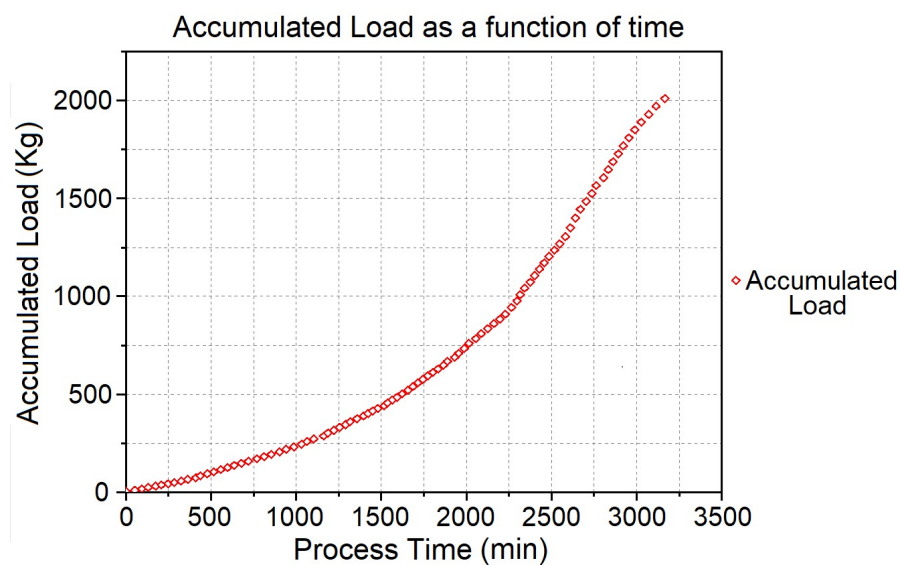**Figure 3.** Flow diagram of the French method for product design

Figure 4. Coal consumption during the firing process

Table I. Characterization of coal and solid combustion products

SAMPLE	% H$_2$O	%Cz	%MV	%CF	%S	CV (Kcal/Kg)	IHL	%C$_{inq}$
COAL	2.57	7.05	43.25	47.14	0.96	5850.00	1.00	-
PSC H1	0.49	91.90	2.36	5.25	0.15	7226.00	0.00	8.90
PSC H2	0.36	91.48	2.12	6.04	0.13	7312,00	0.00	1020

Note: sample H$_2$O: moisture – ASTM D3173; Cz: ashes – ASTM D3174; MV: volatile matter – ASTM D3175; CF: fixed carbon – ASTM D3172; S: sulfur – ASTM D4239; CV calorific value – ASTM D2015; IHL: free swelling index – ASTM D750; C$_{inq}$ unburned coal; PSC: solid combustion products; H1: firebox 1; H2: firebox 2

This table shows that the differences between the percentages of moisture, ashes, volatile matter, and fixed carbon in the solid combustion byproducts are less than 1 %. From these data, it can be deduced that the combustion efficiency of the analyzed fireboxes is similar. Furthermore, the average calorific value of the unburned material increased by 19.52 % compared to the original coal. This behavior explains the formation of char (17). Lastly, 14.59 % of the sulfur contained in the coal was retained in the solid combustion products; we inferred that the remaining percentage was released through gaseous emissions.

3.3.   Characterization of the solid combustion products

The elemental composition (expressed in the form of percentages) was determined via X-ray fluorescence (XRF) analysis (Fig. 5), and the phase distribution was obtained through X-ray diffraction (XRD) (Fig. 6). We found 52.8 % Si, 25.4 % Al, and 6.08 % Fe as major elements, as well as Na, Mg, P, Cl, K, Ca, Ti, Sr, and Pd in lower proportions. The phases identified via XRD were 41.0 % silicon oxide, 42.2 % mullite, and 15.7 % goethite.

The thermal behavior was determined through a differential scanning calorimetry thermogravimetric analysis (DSC-TGA). The thermogram in Fig. 7 presents the mass loss curves as a function of temperature and the energy variation resulting from the phase and compositional changes in the solid combustion residues.

3.4.   Thermal profile of the beehive kiln

The temperature monitoring data, obtained as a function of time, are presented in Fig. 8. These correspond to measurements taken at the dome (CUP), chimney base (CHM), and fireboxes 1 (HNL1) and 2 (HNL2).
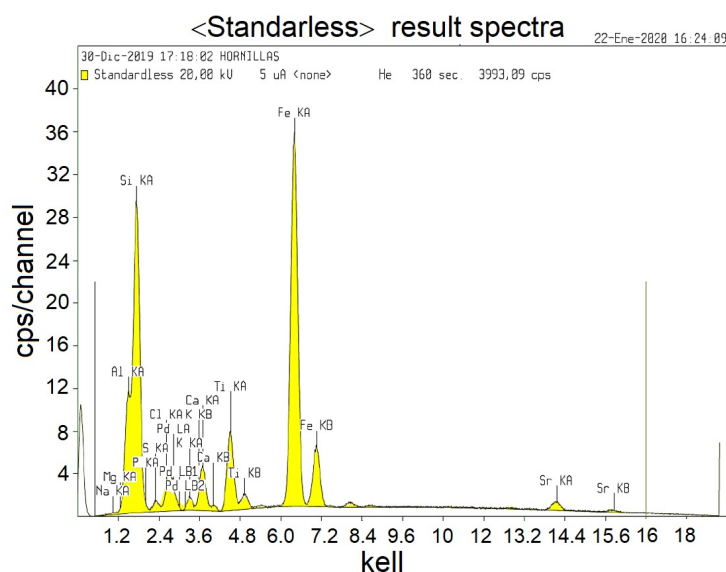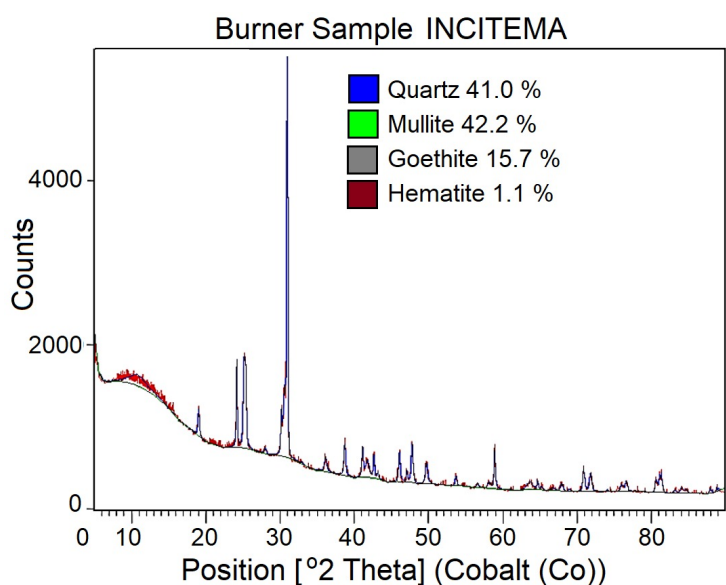
Figure 5. FRX spectrum

Figure 6. XRD diffractogram

3.5. Evolution of emissions and gas

We documented the emissions via photographs for one loading cycle over an average period of 45 min, in order to determine the characteristics of the chimney emissions. This is shown in Fig. **9**.

The results of the gas analysis for six loading cycles—at 45min intervals—are represented by dotted boxes, which enclose the maximum hydrocarbon emission peaks (Fig. **10**) associated with the loading periods. In Fig. **11**, the dotted lines emphasize the ascending regions of the CO and CO_2 curves, which
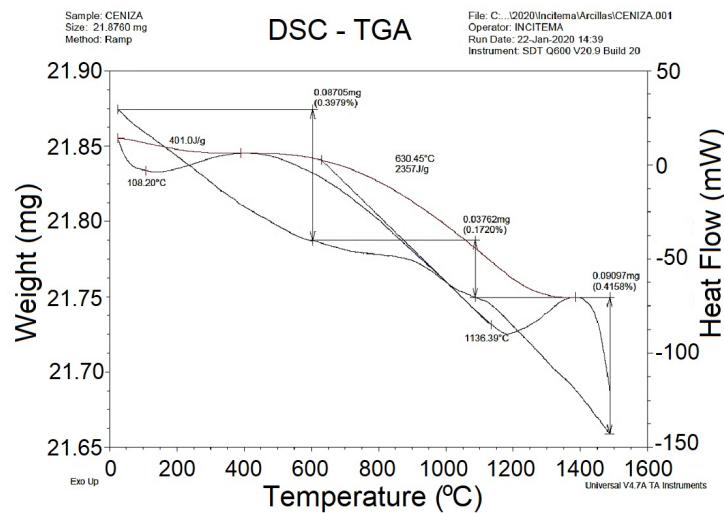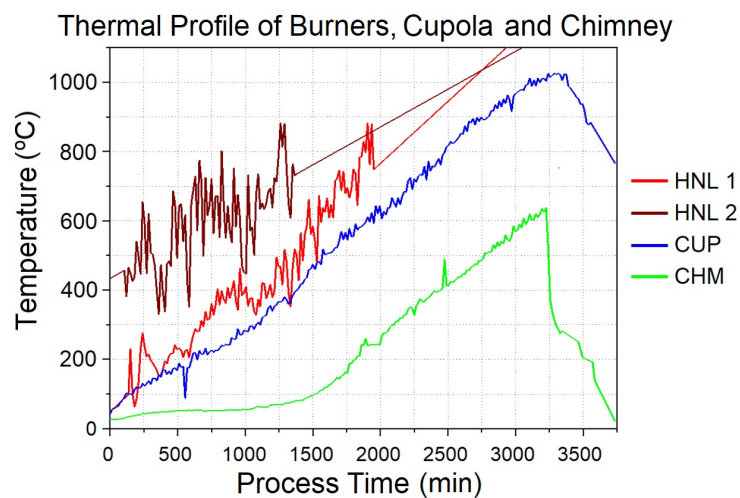
Figure 7. TGA thermogram

Figure 8. Thermal profile of the ceramic firing process in the beehive kiln
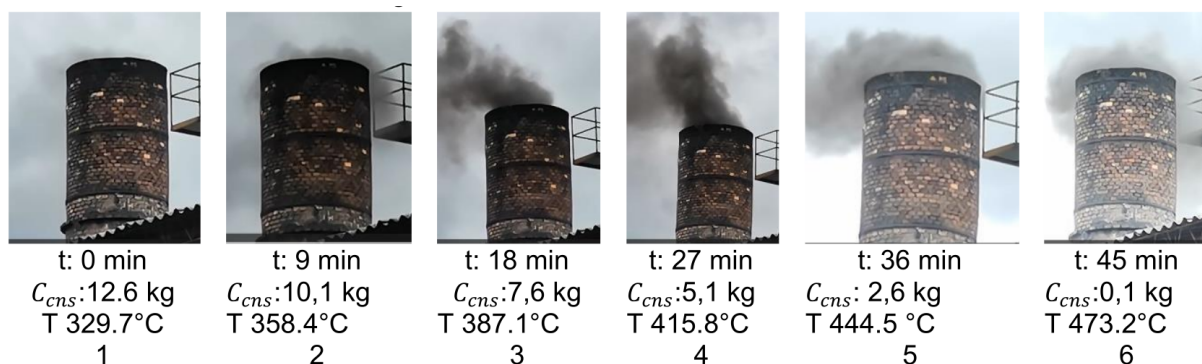

Figure 9. Photographic sequence of chimney emissions for a single loading cycle

contrast with the descending trajectories of O_2. At the end of the process, the reduction in the coal fed to the kiln correlates with the overall emissions reduction.
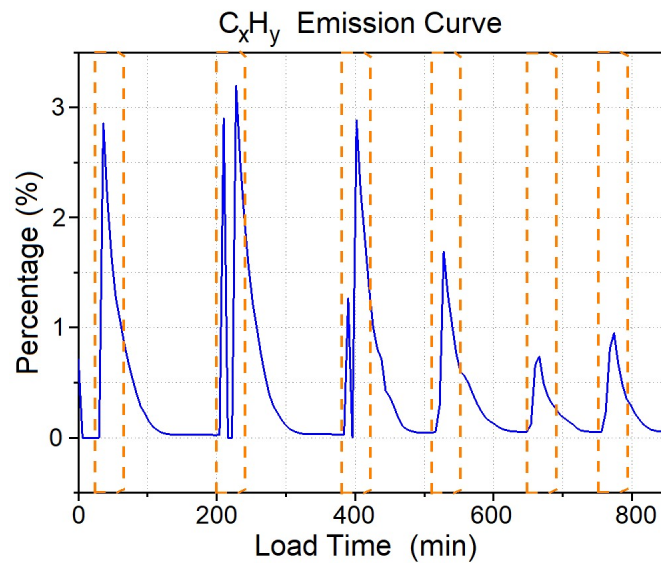
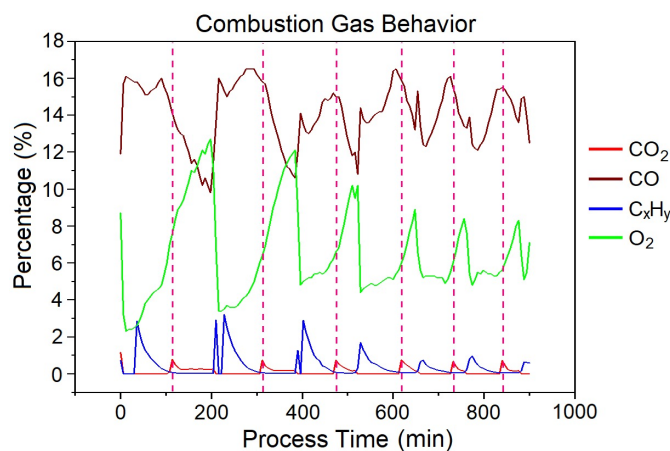

Figure 10. Hydrocarbon emissions plot

Figure 11. Plot of CO_2, CO, CXHY, and O_2 emissions

3.6. Thermodynamic modeling

As a result of the analysis and monitoring of the coal combustion process (12) on a fixed-bed grate (Fig. 2), a thermodynamic model was obtained for the SCMCS-PCV system (Fig. 12). This system consists of a fixed grate equipped with ducts for convective air pre-heating (18), utilizing the heat generated from the exothermic chemical reactions. This mechanism not only recovers heat; it also cools the grate tubes, thereby improving their service life.
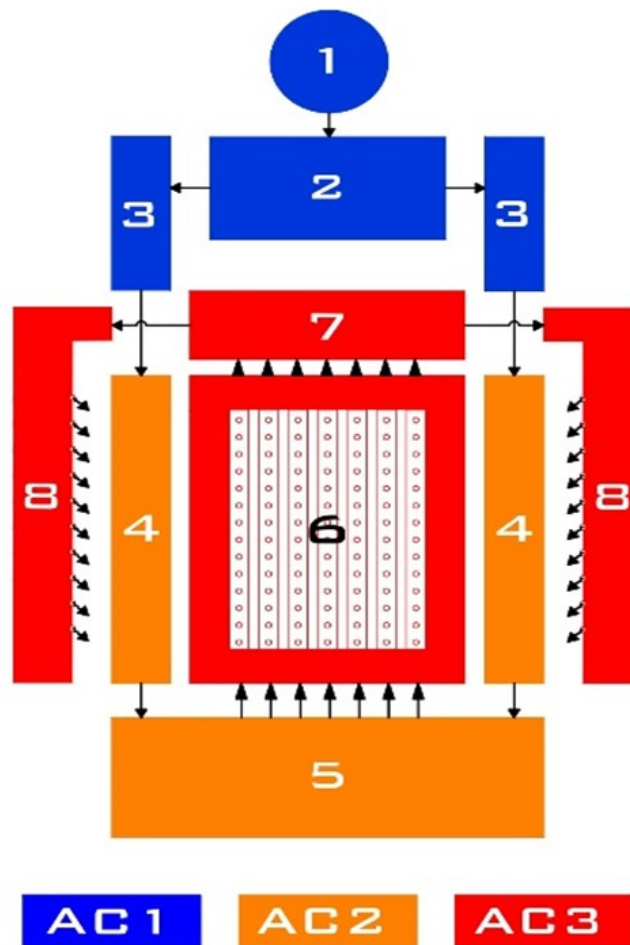
Figure 12. Flowchart of the SCMCS-VPC's thermodynamic model

Conventions

1. Controlled air supply source

2. Air distribution chamber

3. Air distribution ducts

4. Air preheating ducts

5. Pre-heated air distribution chamber

6. Grate for coal combustion with pre-heated air

7. Pre-heated air collector

8. Pre-heated secondary air injector for volatile port- combustion

AC1: Air condition 1 (25 °C)
AC2: Air condition 2 (250 °C)
AC3: Air condition 3 (400 °C)

The thermodynamic model operates as follows. Controlled air is supplied (1) at ambient temperature, which then reaches the air distribution chamber (2), continuing through two conduction sets (3) and the preheating ducts (4) to fill the pre-heated air distribution chamber (5). From this chamber, the air passes through the perforated tubular bars of the fixed-bed grate (6), where part of the flow acts as primary air for coal combustion, while the remaining portion continues towards the pre-heated air collector (7) and is distributed via the injectors as secondary air for volatiles post-combustion (8). The 3D model of the SCMCS-VPC (Fig. 13), derived from thermodynamic modeling, contains a variable-speed fan that delivers the air in a controlled manner. This air is pre-heated in the corresponding chambers by thermo-regulated electric heaters and then supplied to the fixed-bed grate, which consists of the air distribution chamber, the combustion tubes with primary air, and the collector duct. From the collector, the air continues to the secondary air injectors, where it is blown across the fuel load, transversely to the secondary combustion gas stream, to induce the post-combustion of volatiles. The supply of solid carbonaceous material to the grate is managed from a hopper equipped with a dosing system.
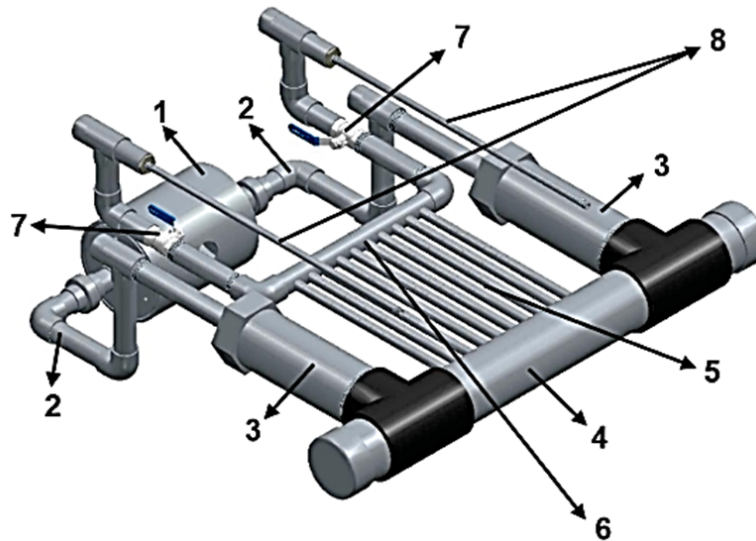

Figure 13. 3D design of the SCMCS-VPC and its components: 1) supply chamber, 2) duct, 3) assisted pre-heating chamber, 4) distribution chamber, 5) grate, 6) collector duct, 7) access ports, 8) secondary air injectors

4. Discussion

Based on the characterization results (Table I), and according to ASTM D388, the coal used can be classified as a low-rank, non-caking sub-bituminous type-A coal (19). This type of coal is also used in the brick industry of several Asian countries (8).

Factors such as the coal composition, the high volatile matter content (43.25 %), the coal particle size (+2 in), open-door combustion, the combustion temperature, air supply deficiency, and the lack

of operational control affected process efficiency and performance (20, 21), resulting in incomplete combustion and the emission of gases, smoke, and particulate matter (soot) through the chimney (Fig. 9), in addition to solid combustion residues (ashes and unburned carbon), which represent energy losses (4, 22).

Fig. 11 shows alternating cycles of maximum and minimum emissions with a decreasing trend as a function of process time. In the gas analysis, CO_2, the main product of combustion, exhibited concentrations between 10 and 16 %. In addition, CO reached 1 %, the C_XH_Y levels were less than 3 %, and no significant emissions of nitrogen oxides (NO_x) were detected, since high temperatures were not reached (17, 23).

According to the literature, at temperatures below 600 °C, alkenes (ethylene, propylene, butene) and aromatics (benzene, toluene, and naphthalene), can be formed, among others (23). These byproducts represent a significant risk to human health and the environment (24, 25).

According to Table I, the char (unburned material), the solid carbonaceous residue that remains after the release of volatile matter, formed due to oxygen deficiency, contains 52.44 % of fixed carbon and exhibits a higher calorific value (7269 kcal/kg), compared to the original coal (5850 kcal/kg), representing an increase of 19.52 %. This high energy value is explained by the fact that char is a carbon-rich matrix (1). Additionally, the mean char content in the ashes is higher than that reported for the boiler combustion process (up to 45 %) (27), which is consistent with a fixed-bed combustion configuration.

The results of the TGA (Fig. 7) show a mass loss equivalent to 0.08705 mg (0.3979 %) within a temperature range of 25-600 °C. Water vaporization was recorded between 25 and 100 °C (28). Based on the proximate analysis of the coal and the XRF results of the ashes (Fig. 5), the presence of S, Na, and Cl was inferred. These elements may be associated with the dehydration (100-200 °C) of sulfates and bicarbonates ($NaHCO_3.5H_2O$) (28). The mass losses between 200 and 400 °C indicate an exothermic behavior due to the combustion of the residual unburned carbon (29). Finally, the mass losses recorded between 400 and 900 °C suggest the fusion of chlorides and the decomposition of carbonates and sulfurates, corresponding to endothermic processes (29). In terms of energy analysis, the behavior between 200 and 400 °C may be due to oxygen absorption into the fuel's porous texture. Furthermore, the rapid mass loss beyond 400 °C indicates the onset of ignition and active combustion (29).

In the thermal profile (Fig. 8), the temperature curves for HNL1 and HNL2 exhibit significant fluctuations, which are explained by the fact that the process involves open-door firebox combustion and is influenced by variable environmental conditions such as relative humidity, ambient temperature, and an irregular air inflow. The temperature profile in the dome (CUP) registers fewer variations, as this is the part of the kiln where heat generated in the fireboxes accumulates for distribution through the ceramic load. The chimney base (CHM) temperature curve reflects an average cooling of 380 °C compared to the maximum temperatures reached in the dome, which are associated with convective

and radiative heat transfer from the flue gases to the ceramic mass during firing. During the first 25 h (1500 min), the gas temperature at the CHM does not exceed 100 °C. After 29 h (1740 min), however, it decreases by approximately 30°C, which can be attributed to the thermal saturation of the firing material.

According to current and emerging trends, the objective is to reduce fuel consumption by up to 30 %, optimize firing times, and minimize pollutant emissions (30), (**?**). The design of the SCMCS-VPC (Fig. **13**) aims to enhance process efficiency and improve the quality of ceramic products (30, 31). The system integrates a coal feeding device and variable-speed blower as key components for animation and process control, along with preheated secondary air injectors to promote volatiles post-combustion.

At the industrial level and in mass production scales, coal combustion systems employing fixed-beds, moving grates, and upward-moving fixed-grates are utilized, wherein the combustion air is preheated to achieve a high-temperature operation. This approach involves the burning of solid fuel with particle sizes between 6 and 50 mm along with the released volatiles (**?**, 16). These design and operation principles were considered as references in the development of the SCMCS-VPC, aiming for improved energy efficiency and reduced environmental impacts.

5. Conclusions

This article presented the design of a 3D model for a solid carbonaceous material combustion system with volatiles post-combustion (SCMCS-PCV) as a technological conversion alternative for beehive kilns equipped with fixed-bed grates.

The monitoring of the ceramic product firing process, conducted at the Maguncia brick industry and the artisan factories in the municipality of Ráquira (Boyacá, Colombia), made it possible to identify the factors affecting the energy efficiency of the sub-bituminous coal used (volatile matter emissions and unburned material), as well as its environmental performance.

The 3D model, derived from the geometric and thermal design, improves the conventional fixed-bed grate combustion process by incorporating a primary air pre- heating system to increase the combustion temperature, as well as a secondary air injection system for volatiles post-combustion. Additionally, the system includes an ash evacuation control mechanism to minimize unburned carbon generation. Thus, the proposed model achieves an increase in energy efficiency and a reduction in the environmental impacts associated with coal combustion.

6. Author contributions

Marco Antonio Ardila-Barragán: project administration, methodology, formal analysis, investigation, writing (review and editing)

7.   Acknowledgments

References

[1] S. Jain, "Development of UNfiRED BRICKS USING INDUSTRIAL WASTE," 2016. [Online]. Available: https://doi.org/10.13140/RG.2.2.23905.51047 ↑3, 15

[2] A. Eser, "Essential brick industry statistics in 2023," ZipDo, 2023. [Online]. Available: https://zipdo.co/statistics/brick-industry/ ↑3

[3] Dirección de Asuntos Ambientales Sectorial y Urbana., L. F. González Herrera, J. I. Pedraza Vega, M. Gaitán Varón, and Corporación Ambiental Empresarial (CAEM), *Portafolio de mejores técnicas disponibles y mejores prácticas ambientales para el sector alfarero y de producción de ladrillo en Colombia.* Bogotá DC, Colombia: Ministerio de Ambiente y Desarrollo Sostenible, 2021. ↑3

[4] C. David and M. Cabeza, "Panorama sobre modelado de eficiencia energética en hornos ladrilleros colombianos", 2023. [Online]. Available: https://www.cdtdegas.com/images/Descargas/Nuestra_revista/MetFlu16/1_Modelado_eficiencia_hornos.pdf ↑3, 15

[5] I. M. Guerrero, E. A. Goldstein, J. H. Stein, H. Acquay, and M. Sarraf, "Introducing energy-efficient clean technologies in the brick sector of Bangladesh," World Bank, 2011. [Online]. Available: https://documents.worldbank.org/en/publication/documents-reports/documentdetail/770271468212375012 ↑3

[6] C. W. Schmidt, "Modernizing artisanal brick kilns: A global need," *Environ. Health Perspect.*, vol. 121, no. 8, pp. A244–A 246, Aug. 2013, https://doi.org/10.1289/ehp.121-A242 ↑3

[7] M. Zavala *et al.*, "Black carbon, organic carbon, and co-pollutant emissions and energy efficiency from artisanal brick production in Mexico," *Atmos. Chem. Phys.*, vol. 18, no. 8, pp. 6023–6037, Apr. 2018. https://doi.org/10.5194/acp-18-6023-2018 ↑3

[8] K. M. ud Darain *et al.*, "Energy efficient brick kilns for sustainable environment," *Desalin. Water Treat.*, vol. 57, no. 1, pp. 105–114, Jan. 2016. https://doi.org/10.1080/19443994.2015.1012335 ↑3, 14

[9] M. R. Riazi and R. Gupta, *Coal Production and Processing Technology*. Boca Ratón, Florida, USA: CRC Press, 2016. ↑3, 6

[10] C. Weyant *et al*., "Brick kiln measurement guidelines: Emissions and energy performance," Aug. 2016. [Online]. Available: https://www.ccacoalition.org/sites/default/files/resources/BC_BrickKilns_GuidanceDocument_Final.pdf ↑3

[11] I. Blasco, J. Ferrero, C. García, and R. González, "Análisis y descripción gráfica del funcionamiento de los hornos cerámicos," 2015. [Online]. Available: https://ceramica.name/img/descargas/Hornos%20ceramicos.pdf ↑3

[12] A. W. Date, *Analytic combustion: With thermodynamics, chemical kinetics, and mass transfer.* Bombay, India: Cambridge University Press, 2011. ↑6, 12

[13] J. M. Samet, "Introduction," in *Air pollution and cancer*, K. Straif, A. Cohen, and J. Samet, Eds. Lyon, France: International Agency for Research on Cancer (IARC), World Health Organization, 2013 ↑6

[14] N. Cross, *Métodos de diseño: estrategias para el diseño de productos*, F. R. Pérez Vázquez, Trad. México DF, Mexico: Limusa Wiley, Grupo Noriega Editores, 2002. ↑6

[15] K.-C. Xie, *Structure and reactivity of coal. A survey of selected Chinese coals*, Beijing, China: SpringerLink, 2015. https://doi.org/10.1007-978-3-662-47337-5 ↑6

[16] V. Raghavan, *Combustion technology: Essentials of flames and burners*. London, UK: John Wiley & Sons Ltd, 2016. ↑6, 16

[17] D. A. Bell, B. F. Towler, and M. Fan, *Coal gasification and its applications.* Oxford, UK: Elsevier, 2011. https://doi.org/10.1016/b978-0-8155-2049-8.10015-4 ↑9, 15

[18] Y. Cengel, *Transferencia de calor y masa: un enfoque práctico*, 3rd ed. México DF, Mexico: McGraw-Hill Interamericana, 2007. ↑12

[19] Servicio Geológico Colombiano, *El carbón colombiano. Recursos, reservas y calidad*, 2nd ed., vol. 32. Bogotá DC, Colombia: Libros del Servicio Geológico Colombiano, 2012. ↑14

[20] Y. Han *et al*., "Different formation mechanisms of PAH during wood and coal combustion under different temperatures," *Atmos. Environ.*, vol. 222, art. 117084, 2020. https://doi.org/10.1016/j.atmosenv.2019.117084 ↑15

[21] T. G. Bridgeman, J. M. Jones, and A. Williams, "Overview of solid fuels, characteristics and origin," in *Handbook of Combustion*, Vol. 4: Solid Fuels, M. Lackner, F. Winter, and A. K. Agarwal, Eds. Weinheim, Germany: Wiley-VCH, 2010, ch. 1, pp. 1-30. https://doi.org/10.1002/9783527628148.hoc055 ↑15

[22] L. F. Velásquez Vallejo, J. F. D. L. C. Morales, J. F. Sánchez Morales, and M. A. Marín Laverde, "Remoción de carbón inquemado de las cenizas volantes producidas en el proceso de combustión de carbón," *Rev. Energ.*, vol. 38, pp. 107–112, Dec. 2007. ↑15

[23] J.-J. Weng, Z.-Y. Tian, Y.-X. Liu, Y. Pan, and Y.-N. Zhu, "Investigation on the co- combustion mechanism of coal and biomass on a fixed-bed reactor with advanced mass spectrometry," *Renew. Energy*, vol. 149, pp. 1068–1076, 2020. https://doi.org/10.1016/j.renene.2019.10.110 ↑15

[24] C. Chen, Q. Yang, R. Zhang, and D. Liu, "Assessment on combustion chemistry of coal volatiles for various pyrolysis temperatures," *J. Energy Inst.*, vol. 104, pp. 22–34, Oct. 2022. https://doi.org/10.1016/j.joei.2022.07.001 ↑15

[25] A. Abbas *et al.*, "Assessment of long-term energy and environmental impacts of the cleaner technologies for brick production," *Energy Rep.*, vol. 7, pp. 7157–7169, Nov. 2021. https://doi.org/10.1016/j.egyr.2021.10.072 ↑15

[26] J. G. Speight, *The chemistry and technology of coal*, 3rd ed. Abingdon, Oxfordshire, UK: Taylor & Francis Group, 2013. ↑

[27] S. V. Vassilev, C. G. Vassileva, and N. L. Petrova, "Thermal behaviour of biomass ashes in air and inert atmosphere with respect to their decarbonation," *Fuel*, vol. 314, art. 122766, Apr. 2022. https://doi.org/10.1016/J.FUEL.2021.122766 ↑15

[28] P. Kumar and B. K. Nandi, "Assessment of combustion characteristics of high ash Indian coal, petroleum coke and their blends for cement industry using TGA," *Cleaner Chem. Eng.*, vol. 5, art. 100091, 2023. https://doi.org/10.1016/j.clce.2022.100091 ↑15

[29] H. Valdes, J. Vilches, G. Felmer, M. Hurtado, and J. Figueroa, "Artisan brick kilns: State-of-the-art and future trends," *Sustainabilty*, vol. 12, no. 18, art. 7724, 2020. https://doi.org/10.3390/su12187724 ↑15

[30] S. M. K. S. Rahman, "Assessment of brick kiln technologies of Bangladesh," MS thesis, Inst. Approp. Tech. (IAT), Bangladesh Univ. Eng. Tech. (BUET), Dhaka, Bangladesh, 2019. ↑16

[31] K. W. Ragland and K. M. Bryden, *Combustion engineering*, 2nd ed. Boca Raton, FL, USA: CRC Press, 2010. ↑16